



# Weibull parameters of Yakuno basalt targets used in documented high-velocity impact experiments

Nakamura, Akiko M.

Michel, Patrick

Setoh, Masato

---

(Citation)

Journal of Geophysical Research E, 112(e2):E02001-E02001

(Issue Date)

2007-02

(Resource Type)

journal article

(Version)

Accepted Manuscript

(URL)

<https://hdl.handle.net/20.500.14094/90000978>



# **Weibull parameters of *Yakuno* basalt targets used in documented high-velocity impact experiments**

by

*Akiko M. Nakamura*<sup>1</sup>,

*Patrick Michel*<sup>2</sup>,

*and*

*Masato Setoh*<sup>1</sup>

<sup>1</sup>Graduate School of Science and Technology, Kobe University, 1-1 Rokkodai-cho, Nada-ku,  
Kobe, 657-8501, Japan

<sup>2</sup>Observatoire de la Côte d'Azur, UMR 6202 Cassiopée/CNRS, BP 4229, 06304 Nice Cedex 4,  
France

Address for correspondence:

Akiko M. Nakamura

e-mail : [amnakamu@kobe-u.ac.jp](mailto:amnakamu@kobe-u.ac.jp)

Graduate School of Science and Technology

Kobe University

1-1 Rokkodai-cho, Nada-ku,

Kobe, 657-8501, Japan

Tel and Fax : +81-78-803-6483

## Abstract

In this paper, we describe our measurements of the Weibull parameters of a specific basalt material, called *Yakuno* basalt, which was used in documented high-velocity impact experiments. The outcomes of these experiments have been widely used to validate numerical codes of fragmentation developed in the context of planetary science. However, the distribution of incipient flaws in the targets, usually characterized by the Weibull parameters, have generally been implemented in the codes with values allowing to match the experimental outcomes, hence the validity of numerical simulations remains to be assessed with the actual values of these parameters from laboratory measurements. Here, we follow the original method proposed by Weibull in 1939 to measure these parameters for this *Yakuno* basalt. We obtain a value of the Weibull modulus (also called shape parameter)  $m$  in the range 15-17 with typical error about 1.0 for each different trial. This value is larger than the one corresponding to simulation fits to the experimental data, generally around 9.5. The characteristic strength, which corresponds to 63.2 % of failure of a sample of similar specimens and which defines the second Weibull or scale parameter, is estimated to be 19.3-19.4 MPa with typical error about 0.05 MPa. This parameter seems not sensitive to the different loading rates used to make the measurements. A complete database of impact experiments on basalt targets, including both the important initial target parameters and the detailed outcome of their disruptions, is now at the disposal of numerical codes of fragmentation for validity test.

Keywords: basalt; fractures; impact experiments; tensile strength; Weibull distribution: small bodies

## 1. Introduction

The aim of this paper is to present the measurements of important material parameters, the Weibull constants, of basalt targets used in the high-velocity impact experiments performed by *Nakamura and Fujiwara* [1991]. This basalt is called *Yakuno* basalt, from the name of an area of Kyoto where it was extracted. The outcomes of these experiments have been documented in details and have thus been used to validate state-of-the-art numerical codes of solid body disruption in the context of planetary science [e.g., *Benz and Asphaug*, 1994].

It is well known that real materials, such as rocks, are in general inhomogeneous and have random flaw distribution. Therefore, their fracture is influenced by the heterogeneous structure of the material and such heterogeneity has to be implemented in numerical codes of rock fragmentation to simulate the fracture process correctly. In particular, a size effect has been observed and its existence reflects the occurrence of a statistical process having its roots at microscopic level. This effect was apparently discovered by Leonardo da Vinci [e.g., *Parsons*, 1939; *Lund and Byrne*, 2000] who tested iron wires and remarked that shorter wires could support a greater weight, in contrast with the classical theory of mechanics of materials. This phenomenon has given rise to probabilistic fracture models for the description of strength behavior of brittle solids.

Numerical simulations of brittle solid break-ups generally use a fracture model based on the nucleation of incipient flaws [e.g., *Melosh et al.*, 1992; *Benz and Asphaug*, 1994]. In such a model, the density number of flaws in a rock that activate at a stress not greater than  $\sigma$  is given by the two-parameter Weibull distribution [*Weibull*, 1939; *Jaeger and Cook*, 1969], as:

$$n(\sigma) = K \left( \frac{\sigma}{\sigma_N} \right)^m, \quad (1)$$

where  $K$  and  $m$  are constant and  $\sigma_N$  is a characteristic strength (see Sec. 2). Numerical codes usually consider the strain, instead of the stress, to model this distribution which is then expressed as:

$$N(\varepsilon) = k\varepsilon^m, \quad (2)$$

where  $N$  is the number density of flaws having failure strains smaller than  $\varepsilon$ . Hooke's law is generally used to relate both expressions, i.e.  $\sigma = E\varepsilon$ , where  $E$  is the Young modulus of the material. This incipient flaw distribution is typically assumed to arise from irregularities in the cooling history of the rock, and from crystal lattice imperfections. This concept argues that a specimen, considered to be composed of  $N$  elements or links, will break as its weakest element breaks. It is clear that the outcome of impact simulations depends greatly on the choice of the Weibull constants. Indeed, the activation stress  $\sigma_{min}$  corresponding to the most probable weakest flaw in a target of volume  $V$  is derived from  $n(\sigma_{min}) \equiv 1/V = K(\sigma_{min}/\sigma_N)^m$ ; i.e.:

$$\sigma_{min} = \sigma_N (KV)^{-1/m}. \quad (3)$$

The threshold for failure  $\sigma_{min}$  thus goes with the  $-3/m$  power of radius of a spherical target. For reasons not yet understood, some studies suggest that a value of  $m$  about 6 may be favored by nature [Housen and Holsapple, 1999]. However, values of  $m$  as high as 57 and as low as 3 are reported for rocks in the literature, sometimes for the same kind of rock. For instance, Vardar and Finnie [1977] report a value of 2.9 for basalt, and of 3-4 for limestone, while Asphaug *et al.* [2002] indicate values around 9.5 for basalt and 57 for limestone.

The values often given for basalt are about 9-9.5 but they are usually determined from simulations fits to laboratory data (see below). Moreover, there is a wide variety of basalts, granites and other materials, so that the values that may be measured for a specific kind of basalt may not represent the ones characterizing the basalt used in another experiment. For instance, a value of  $m$  equal to 9.5 is quoted in Asphaug et al. [2002] and has been derived *indirectly* from some measurements of the dynamic strength and fracture properties of a particular kind of basalt called *Dressler basalt* performed by Lindholm et al. [1974].

Therefore, in principle, impact experiments on a given kind of solid material should be accompanied with the measurement of the Weibull parameters for this material and these measured values should in turn be used in the numerical runs aimed at reproducing these experiments. Otherwise, the validation of a numerical code cannot be considered as fully guaranteed if the Weibull constants are arbitrarily chosen to match the experiments. For instance, Benz and Asphaug [1994] developed a 3D hydrodynamical code based on the SPH (Smooth Particle Hydrodynamics) numerical technique, which includes a model of brittle failure. This SPH hydrocode is considered as the state-of-the-art numerical code used to perform simulations of solid body disruptions, such as asteroid break-ups. Combined with a N-body gravitational code to take into account gravitational phenomena at large scales, it has successfully reproduced the main properties of asteroid families, which are each composed of large bodies (km-size at least) who share the same orbital and spectral properties and who originated from the disruption of a larger parent body [e.g., Michel et al., 2001, 2003, 2004]. However, its validation at small scales relies on Weibull parameters for basalt, which were set to best match the impact experiments of Nakamura and Fujiwara [1991] on basalt targets, since the Weibull parameters for *Yakuno* basalt were not measured at the time Benz and Asphaug performed their numerical test. Such a validation is not totally satisfactory, as it is not proven that the use of the actual values in the simulations would lead to the same success.

The high-velocity impact experiments performed by *Nakamura and Fujiwara* [1991] on basalt targets are a good test for the numerical codes, because their outcomes have been accurately measured, in particular concerning the size and ejection velocity distributions of the fragments. However, at the time when these experiments had been prepared, the necessity to measure the Weibull parameters of the targets did not appear crucial, so they have been left unknown. Fortunately a few targets prepared for these experiments have not been disrupted yet, hence we can use them to measure those fundamental parameters. The knowledge of both crucial material parameters like the Weibull constants of the targets and the outcome properties of their disruptions in different impact conditions would make of these experiments a complete database which can be used to validate the numerical codes.

The estimate of the Weibull parameters presented in this paper relies on the method proposed by Weibull himself in 1939 (see also *Weibull*, 1951), which is used in many studies related to the rock fracture process and material strength. It starts from a probabilistic fracture model for the description of the strength behavior of brittle solids, based on the Weibull distribution (see Sec. 2). An estimator is used, which is assumed to provide the least biased values of the Weibull parameters for a number of specimens less than 50. It is thus the appropriate method in our case, as only a few pieces of basalt samples remain from the experiments of 1991. Of course, small numbers of specimens can always imply large uncertainties, but we claim that the number of specimens that we use is enough to reach our objectives.

The reminder of this paper can be described as follows. In Section 2, we recall the definition of the Weibull distribution and the physical meaning of the two key parameters. Section 3 describes the measurements performed on the samples while Section 4 presents the results of these measurements and the derivation of the Weibull parameters in the form that

can directly be implemented in numerical simulations. Section 5 exposes the conclusion and perspectives.

## 2. The Weibull method

For failure under essentially static loads and tensile states of stress, the inherent flaws in a brittle solid may be regarded as links in a chain with failure of the part being governed by failure of the weakest link. This is the approach proposed by *Weibull* [1939, 1951] who developed it to relate the variability in strength of nominally identical specimens to the effect of specimen size and stress distribution on strength. Thus, the Weibull distribution applies when there are multiple similar opportunities to fail and the interest is in the first failure. It is sometimes called the weakest-link-in-the-chain distribution. Its application goes from the strength of steel to life data [*Weibull*, 1951].

Different estimators are generally used to calculate the probability of failure  $P_i$  of the  $i$ th strength. The following estimator is assumed to lead to the least biased values of the parameter  $m$  of a Weibull distribution function for number of specimens  $N$  less than 50 [e.g., *Asloun et al.*, 1989; *Zinck et al.*, 2002]:

$$P_i = \frac{(i - 0.5)}{N} \quad (4)$$

Note that some authors [e.g., *Dirikolu et al.*, 2002] used the median rank of  $\sigma(i)$  as the estimator. Calling it  $M$  to avoid confusion with the previous estimator, it is defined as:

$$M_i = \frac{i - 0.3}{N + 0.4} \quad (5)$$

For completeness, we will give the values obtained with both estimators.

The distribution function (cumulative probability of failure) given by Weibull is the following:

$$P(\sigma) = 1 - \exp \left[ - \left( \frac{\sigma}{\sigma_N} \right)^m \right] \quad (6)$$

The parameters  $m$  and  $\sigma_N$  are often called shape and scale, respectively. The following transformation of this equation is a useful tool for fitting the experimental data to obtain the value of shape and scale parameters:

$$\ln \left[ \ln \left( \frac{1}{1 - P(\sigma)} \right) \right] = m \ln(\sigma) - m \ln(\sigma_N) \quad (7)$$

The dependence of  $\ln[-\ln(1-P)]$  vs.  $\ln(\sigma)$  is linear, with a slope equal to  $m$ , if the failure is governed by one type of defect, which can be assumed to be the case for basalt material. This is the advantage of the Weibull analysis: it provides a simple and useful data plot. Moreover, the slope of the line,  $m$ , provides a clue to the physics of the failure. It gives an indication of the degree of homogeneity within the material. Higher values of  $m$  indicate that flaws are more evenly distributed throughout the material, and consequently, the strength is nearly independent of the length. Lower values of  $m$  indicate that flaws are fewer and less evenly distributed, causing greater scatter in strength. The characteristic stress  $\sigma_N$  is the stress at which 63.2 % of the units will have failed.

Another crucial advantage of Weibull analysis is the ability to provide reasonably accurate failure analysis and failure forecasts with extremely small number of specimens. This is why it is often used in industry, for instance in aerospace safety problems [e.g., *Abernethy*, 2000]. In our case, it is also appropriate, as we do not require an accuracy as high as the one required for industrial purposes and only a few basalt targets used in the 1991 experiments still exist.

### 3. Method of measurement

Disc-shaped specimens were cut from an intact 8 cm diameter basalt target that is one of the leftovers of the impact experiments of *Nakamura and Fujiwara* [1991] and *Nakamura* [1993]. All the disks were cut out with their symmetry axis being oriented in the same direction in the original target. Each specimen has a diameter equal to 9.98(+/-0.02) mm, and a thickness of 5.00(+/-0.03) mm. The dimensions were measured with a resolution of 0.01 mm and the scatters among the specimens were within 0.04 mm for the diameter and 0.06 mm for the thickness. The volume  $V$  of our specimens is thus about 391 mm<sup>3</sup>. Tensile strengths were measured by diametral compression of the discs, using a method equivalent to the Brazil disc test [*Mellor and Hawkes*, 1971] with four different loading rates: 0.035, 0.07, 1, and 14 mm/min. Each specimen was stood on its lateral side with its disk surface aligned with the vertical axis of a compressive testing machine installed at Kobe University in Japan. The uncertainty of the applied force was within 0.05%. The specimens were broken along the vertical axis decisively and into two major pieces and small fragments. The tensile stress  $\sigma$  at failure was calculated from the applied force,  $S$ , by the expression  $\sigma = 2S/(\pi dl)$ , where  $d$  and  $l$  are the diameter and thickness of the specimen, respectively.

The results from the four measurements at different loading rates are reported in Table 1.

### 4. Results and discussion

#### 4.1. Determination of the Weibull parameters

We ranked the  $N$  recorded stresses at failure by ascending order ( $i=1, 2, \dots, N$ ) and assigned the cumulative probabilities of failure according to Eq. (4) or Eq. (5). Figure 1 shows the probability given by Eq. (4) as a function of the failure tensile stress. The Weibull parameters  $m$  and  $\sigma_N$  were determined for each loading rate by fitting the data points with the two-parameter Weibull distribution given by Eq. (6) or its linearized version (Eq. (7)). The results are summarized in Table 1.

Numerical simulations of rock fragmentation often use the Weibull distribution in its form related to activation strain rather than stress given by Eq. (2) and the Weibull parameters are the parameters  $m$  and  $k$  in the corresponding expression. The parameter  $k$  (in units of  $\text{m}^{-3}$ ) is related to the classical scale parameter  $\sigma_N$  by using Hooke's law:  $k = (1/V)(E/\sigma_N)^m$ , where  $V$  is the volume of our specimens. Therefore, for practical use, the values of  $k$  associated with  $\sigma_N$  are also indicated in Table 1 for the two lowest loading rates for which Weibull's approach is valid (see Sec. 4.2.2). The value of the Young modulus  $E$  is  $5.32 \times 10^4$  MPa and has been calculated from the measurements of S-wave and P-wave velocities of this same *Yakuno* basalt by *Takagi et al.* [1984], who also provided a value of the compressive strength of 160 MPa.

## 4.2 Discussion

### 4.2.1 Measurements at high loading rates

Starting from a lower loading rate of 0.07 mm/min, the results in Table 1 indicate an increase of the value of  $m$  with the loading rate. Conversely, the characteristic tensile strength  $\sigma_N$  does not monotonically increase with the loading rate, which is expected in the classical model of crack growth in rocks developed by *Grady and Kipp* [1980]. However, the

dependence of  $m$  on the loading rate is still related to the process of crack growth in some way. Indeed, Figure 2 shows the linearized version of Eq. (6), expressed by Eq. (7). The Weibull modulus  $m$  is the slope and the nominal strength  $\sigma_N$  is obtained from the  $\ln[-\ln(1-P)] = 0$  intercept. This figure shows the results using the estimator  $P$  given in Eq. (4) but the same applies to the estimator  $M$  of Eq. (5). The data obtained with the two highest loading rates (1 mm/min and 14 mm/min) fit poorly with the two-parameter Weibull model. In particular, the lines are curved as if there was a truncation at small stresses of failure for these loading rates.

In fact, only in the case of failure under essentially static loads (below a certain threshold of the loading rate) can the incipient flaws be regarded as links in a chain of failure of the part being governed by the weakest link, which is at the basis of Weibull's approach. Conversely, under short duration tensile loading (high loading rates), a single crack can travel only a limited distance in the time of loading and this may not be enough to produce a complete separation of the part. Thus, the weakest link approach may not be appropriate anymore since many cracks may have to initiate before final separation occurs, and the propagation rather than the initiation phase of fracture may be the dominant one. The two greatest loading rates that we applied may thus be too high to be described by the weakest link approach.

The fact that the deviation from a straight line (the Weibull fit) results in a higher variation of the Weibull modulus, while the scale parameter is much less affected is consistent with the interpretation of the scale parameter as a “mean” strength, which is less sensitive than the modulus, which characterizes the uniformity of the flaw distribution and thus the distribution of strength values.

Note that in the case of the 1 mm/min loading rate, the data are shown using 16 specimens. The measurements have also been done for 9 additional specimens. Since their

dimensions were determined with a poorer resolution, 0.05 mm instead of 0.01 mm, we decided to disregard them for consistency in our final analysis. For information we show on Figure 3 the results obtained with and without these 9 specimens taken into account. One can see that the slope of the line (and thus, the value of  $m$ ) is almost the same in both cases. However, even if the line tends also to be curved when the 9 additional specimens are included, a data point appears, which belongs to these specimens, at the low strength end of the distribution and clearly detaches from the curved line. One possible explanation for this data point could be the presence of some unusual large defects in the corresponding specimen, as microscopic 2D images of some specimens have indicated that a few of them contain unusually large pores, which may enhance their breaking at low stress values even at high loading rates. We also estimated the Weibull parameters using the measurements obtained with these 9 specimens only and found a value of  $m$  around 21.7 (+/-1.6) and a value of  $\sigma_N$  around 18.98 (+/-0.05) MPa. Therefore, even considering only those specimens with less well determined dimensions, we obtain a value of  $m$  greater than the values obtained at lower loading rates (so, the tendency of an increase of  $m$  with the loading rate holds true) and the characteristic strength is similar to the ones obtained with the other specimens (and other loading rates).

#### 4.2.2 Measurements at loading rates adapted to Weibull's approach

In order to obtain reliable values of the shape parameter  $m$  we need to make the measurements at loading rates close enough to static loads and thus appropriate to the weakest link concept. In the range of loading rates for which Weibull's model is adapted, the value of  $m$  should in principle remain of the same order of a measurement at a given loading rate to another one at another loading rate. This value would then characterize the actual Weibull

parameter  $m$  of our basalt targets. Initially, we made one measurement at a loading rate of 0.07 mm/min and obtained a value of  $m$  in the range 15-16 (see Table 1), depending on the estimator. We were already confident that this loading rate was in the appropriate range for Weibull's approach, as the data nicely fit with a straight line (see Figs. 2 and 3). As a check, we made another measurement at a lower loading rate (0.035 mm/min) with our remaining specimens and we obtained a value of  $m$  of the same order, even slightly higher (16-17) than the previous one. This makes us confident that these loading rates are below the maximum threshold appropriate to Weibull's approach, as the values of  $m$  are similar, and as there is no systematic increase with the loading rate (actually we observe a slight decrease which is probably statistically irrelevant). Moreover, although the number of specimens used for each measurement was limited, the linear fits are seen to be a reasonable representation of the data, including the all-important low-strength "tail" (see Fig. 4). As represented on Figure 5, the two estimators that we used do not lead to large differences in the values of  $m$  (given the accuracy we are looking for), and we let the reader decide which of the two gives a more reliable estimate. We thus believe that a value of  $m$  in the range 15-17 should be used in numerical runs aimed at reproducing the impact experiments made with these basalt targets. Concerning the parameter  $k$ , which is generally used in numerical codes and set to a value of the order of  $10^{30} \text{ cm}^{-3}$  to match impact experiments, our measurements lead to a value in the range  $10^{51}$ - $10^{59} \text{ cm}^{-3}$ , depending on the choice of the estimator.

## 5. Conclusion

The Weibull parameters of a specific basalt material, called *Yakuno* basalt, which has been used in previous high-velocity impact experiments [Nakamura and Fujiwara, 1991] have been characterized by applying Weibull's approach to a sample of specimens extracted from remaining basalt targets. From our four measurements at different loading rates, we

conclude that the two highest loading rates used are not appropriate to Weibull's approach for determining the incipient flaw distribution, which is based on the weakest-link-in-the-chain concept, as they are probably well above the static load appropriate to this approach.

Conversely, a fit of the data with a two-parameter Weibull distribution appears satisfying for the two lowest loading rates. Moreover, these fits lead to similar values of the Weibull parameters, while they give very different values from one rate to the other at higher rates. This makes us confident that the Weibull parameters obtained from our measurements at the two lowest rates are the ones probably characterizing the actual flaw distribution of this *Yakuno* basalt. We thus propose that a value of  $m$  in the range 15-17 and a characteristic strength about 19.33-19.43 MPa (which implies a value of the  $k$  parameter in the range  $10^{51}$ - $10^{59}$  cm<sup>-3</sup>) should be used in numerical simulations aimed at reproducing the documented impact experiments performed by *Nakamura and Fujiwara* [1991] on this same *Yakuno* basalt. Interestingly, *Benz and Asphaug* [1994] remarked that as long as the value of the ratio  $\ln(k V)/m$  is equal to 8.33 (+/-0.2), their simulations reproduce successfully the core mass fraction found in those experiments. Note that replacing  $k$  by its expression indicated in the caption of Table 1, this ratio becomes  $\ln(E/\sigma_N)$ . The value of the Young modulus  $E$  being known for this material, fixing this ratio implies that the core formation is governed by tensile stresses, as the value of  $\sigma_N$  sets the mass fraction in the core. Thus, in catastrophic impacts the requirement that this ratio must keep a fixed value around 8.33 to get the same core implies that the core is formed essentially by crack growth due to tensile stress. This probably marks the difference with the regime of cratering impacts, as failure criteria based on shear and compression are also certainly relevant in this regime. The values of the Weibull parameters obtained by our measurements together with the volume of 6 cm diameter spheres used in the previous impact experiments result in this ratio going from 8.24 to 8.30, which is in the range indicated by *Benz and Asphaug* [1994]. Therefore it may be that numerical simulations will

still find the correct answer using the measured values, and this will be checked in a close future.

These measurements along with these documented impact experiments provide a more complete database of impacts on basalt targets, which open a new area of investigations. Indeed, future projects will consist of making impact experiments with other kinds of materials and measuring for each considered material, both important initial material parameters, such as the Weibull constants, and the outcomes of impact events in terms of size and velocity distribution of the fragments. It is only with the elaboration of such complete databases for different materials that our understanding of the physics of impact processes and our ability to reproduce them with numerical simulations will improve in a reliable way.

## Acknowledgements

We are grateful to A. Fujiwara for allowing us to break the leftover basalt targets for our measurements. We also thank D. Davis and L. Chambers for their constructive reviews. P.M. acknowledges financial support from the Japan Society for the Promotion of Science (JSPS) and the French Programme Nationale de Planétologie (PNP) 2005-2006. This work was supported by “The 21<sup>st</sup> Century COE Program of the Origin and Evolution of Planetary Systems.” of the Ministry of Education, Culture, Sports, Science and Technology (MEXT), Japan.

## References

Abernethy, R.B. (2000), *The New Weibull Handbook, Reliability & Statistical Analysis for Predicting Life, Safety, Survivability, Risk, Cost and Warranty Claims*, 4th ed., Abernethy, North Palm Beach.

Asloun, E.I.M., J.B. Donnet, G. Guilpain, M. Nardin, and J. Schultz (1989), On the estimation of tensile strength of carbon fibres at short lengths, *J. Mat. Sci.*, 24, 3504-3518.

Asphaug, E., E.V. Ryan, and M.T. Zuber (2002), Asteroid interiors, in *Asteroid III*, edited by W.F. Bottke Jr et al., pp. 463-484, The Univ. of Arizona Press, Tucson.

Benz, W., and E. Asphaug (1994), Impact simulations with fracture. I-Method and tests, *Icarus*, 107, 98-116.

Benz, W., and E. Asphaug (1999), Catastrophic disruptions revisited, *Icarus*, 142, 5-20.

Dirikolu, M.H., A. Aktas, and B. Birgören (2002), Statistical analysis of fracture strength of composite materials using Weibull distribution, *Turkish J. Eng. Env. Sci.*, 26, 45-48.

Grady, D. E., and M. E. Kipp (1980), Continuum modelling of explosive fracture in oil shale, *Int. J. Rock Mech. Min. Sci. Geomech. Abstr.*, 17, 147-157.

Housen, K.R., and K.A. Holsapple (1999), Scale effects in strength dominated collisions of rocky asteroids, *Icarus*, 142, 21-33.

Jaeger, J.C., and N.G.W. Cook (1969), *Fundamentals of Rock Mechanics*, Chapman and Hall, London.

Lindholm, U.S., L.M. Yeakley, and A. Nagy (1974), The dynamic strength and fracture properties of Dressler basalt, *Int. J. Rock Mech. Min. Sci. Geomech. Abstr.*, *11*, 181-191.

Lund, J.R., and J.P. Byrne (2000), Leonardo da Vinci's tensile strength tests: implications for the discovery of engineering mechanics, *Civil. Eng. And Env. Syst.*, *00*, 1-8.

Mellor, M., and I. Hawkes (1971), Measurement of tensile strength by diametral compression of discs and annuli, *Eng. Geol.*, *5*, 173-225.

Melosh, H.J., E.V. Ryan, and E. Asphaug (1992), Dynamic fragmentation in impacts: Hydrocode simulations of laboratory impacts, *J. Geophys. Res.*, *97*(E9), 14735- 14759.

Michel, P., W. Benz, P. Tanga, and D.C. Richardson (2001), Collisions and gravitational reaccumulation: Forming asteroid families and satellites, *Science*, *294*, 1696-1700.

Michel, P., W. Benz, and D.C. Richardson (2003), Fragmented parent bodies as the origin of asteroid families, *Nature*, *421*, 601-611.

Michel, P., W. Benz, and D.C. Richardson (2004), Catastrophic disruption of asteroids and family formation: a review of numerical simulations including both fragmentation and gravitational reaccumulations, *Planet. Space Sci.*, *52*, 1109-1117.

Nakamura, A. and A. Fujiwara (1991), Velocity distribution of fragments formed in a simulated collisional disruption, *Icarus*, 92, 132-146.

Nakamura, A. (1993), Laboratory studies on the velocities of fragments from impact disruptions, *The Institute of Space and Astronautical Science Report No. 651*, 90 pp., Kanagawa, Japan.

Parsons, W.B. (1939), Engineers and Engineering in the Renaissance, *MIT Press*, 661 pp, Cambridge, MA.

Takagi, Y., H. Mizutani, and S.I. Kawakami (1984), Impact fragmentation experiments of basalt and pyrophyllites, *Icarus*, 59, 462-477.

Vardar, Ö, and I. Finnie (1977), The prediction of fracture in brittle solids subjected to very short duration tensile stresses, *Int. Journ. of Fracture*, 13, 115-131.

Weibull, W. (1939), A statistical theory of the strength of materials, *Ingvetensk. Akad Handl.*, 151, 1-45.

Weibull, W. (1951), A statistical distribution function of wide applicability, *J. Appl. Mech.*, 18, 293-297.

Zinck, P., J.F. Gérard, and H.D. Wagner (2002), On the significance and description of the size effect in multimodal fracture behavior. Experimental assessment on E-glass fibers, *Engin. Fracture Mech.*, 69, 1049-1055.

## Figure captions

Figure 1: Failure probability, using the estimator  $P$ , as a function of the applied stress  $\sigma$  (MPa).

The points indicate the measured values, whereas the curves show the fits with the Weibull parameter values reported in Table 1. Data from four loading rates indicated on the plot have been used.

Figure 2: Same as Figure 1, but the cumulative probability of failure is transformed in its linear form provided by Eq. (7).

Figure 3: Same as Figure 2 showing only the measurements made at a loading rate of 1 mm/min. In addition to the data set containing 16 specimens, a second data set containing 25 specimens is shown. This second data set includes the measurements with the same 16 specimens as the first one, as well as 9 additional specimens whose dimensions have been determined with less accuracy (see text for details). The slopes of the two curves are similar. However, the second data set cannot be used for general purposes as it mixes specimens whose dimensions have not been measured with a same accuracy.

Figure 4 : Same as Figure 2, but showing only the data from the two lowest loading rates for which Weibull's approach is appropriate. The slope of each line corresponds to the Weibull modulus  $m$  at the corresponding loading rate. It is equal to  $17.2 \pm 1.4$  and  $16.3 \pm 0.9$  for 0.035 mm/min and 0.070 mm/min, respectively. Thus, both loading rates lead to similar values of the modulus.

Figure 5 : Linear form of the cumulative probability of failure obtained with a loading rate of 0.070 mm/min. The fits obtained for the two estimators  $P$  (Eq. (4)) and  $M$  (Eq. (5)) are shown. The Weibull modulus  $m$  given by the slope of each line is equal to  $16.3 \pm 0.9$  and  $15.0 \pm 0.8$  from the estimator  $P$  and  $M$ , respectively.

Table 1. Weibull parameters of the *Yakuno* basalt derived from measurements at different loading rates. The results obtained with the two estimators  $P$  and  $M$  described in the text (see Sec. 2) are indicated. The parameter  $k$  (in  $\text{cm}^{-3}$ ) is the Weibull parameter in Eq. (2). Its value is only computed for the measurement at the loading rates for which the Weibull model applies (see Sec. 3.2). It is defined by  $k=(I/V)(E/\sigma_N)^m$ , where  $V$  is the volume of our specimens ( $0.391 \text{ cm}^3$ ). The scale parameter  $\sigma_N$  is given in MPa and the Young modulus  $E$  is equal to  $5.32 \times 10^4 \text{ MPa}$ .

Loading rate [mm/min] (number of specimens)	$P$			$M$		
	$m$	$\sigma_N$	$k$	$m$	$\sigma_N$	$k$
0.035 (13)	17.2+/-1.4	19.42+/-0.05	$3.43 \times 10^{59}$	15.9+/-1.3	19.43+/-0.05	$1.16 \times 10^{55}$
0.07 (11)	16.3+/-0.9	19.34+/-0.06	$2.96 \times 10^{56}$	15.0+/-0.8	19.36+/-0.06	$9.84 \times 10^{51}$
1 (16) <sup>a</sup>	26.6+/-3.6	18.79+/-0.07	-	25.1+/-3.2	18.81+/-0.07	-
14 (8) <sup>a</sup>	39.3+/-7.7	20.12+/-0.07	-	35.8+/-6.6	20.14+/-0.07	-

<sup>a</sup>See Sec. 4.2.1 for more information about the measurements at high loading rates.

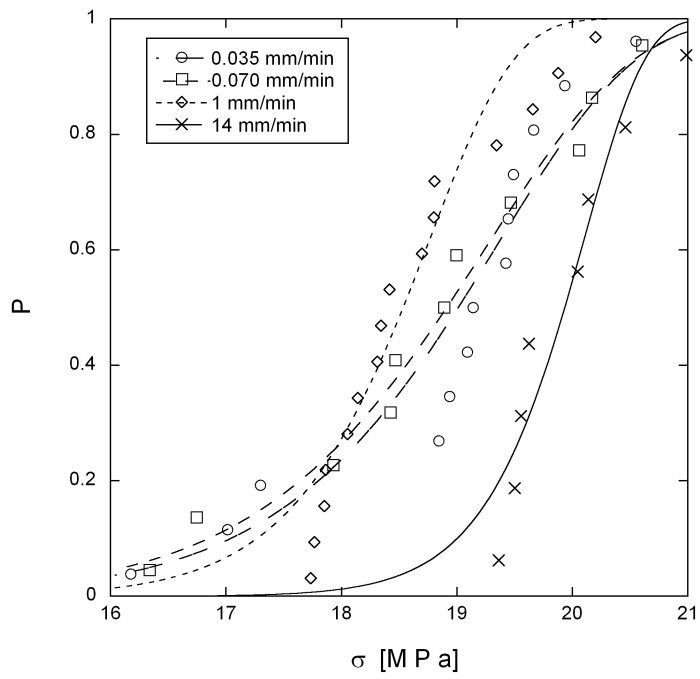


Figure 1: Failure probability, using the estimator  $P$ , as a function of the applied stress  $\sigma$  (MPa).

The points indicate the measured values, whereas the curves show the fits with the Weibull parameter values reported in Table 1. Data from four loading rates indicated on the plot have been used.

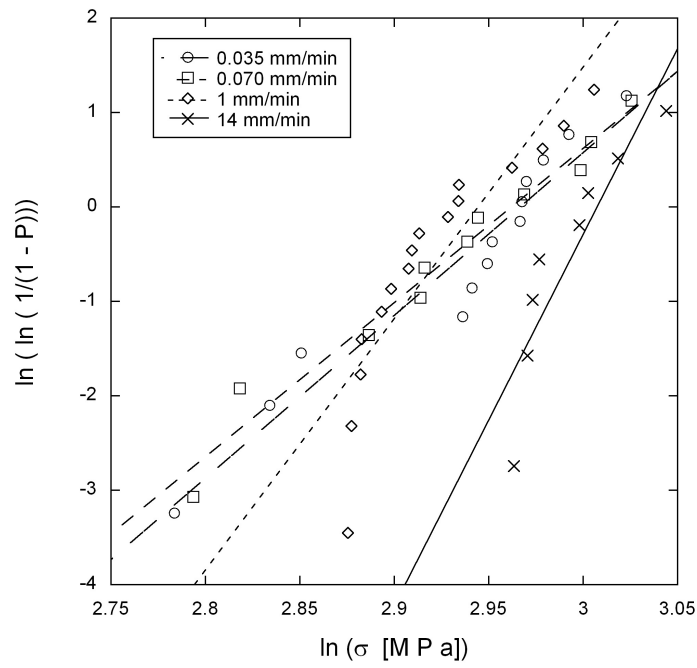


Figure 2: Same as Figure 1, but the cumulative probability of failure is transformed in its linear form provided by Eq. (7).

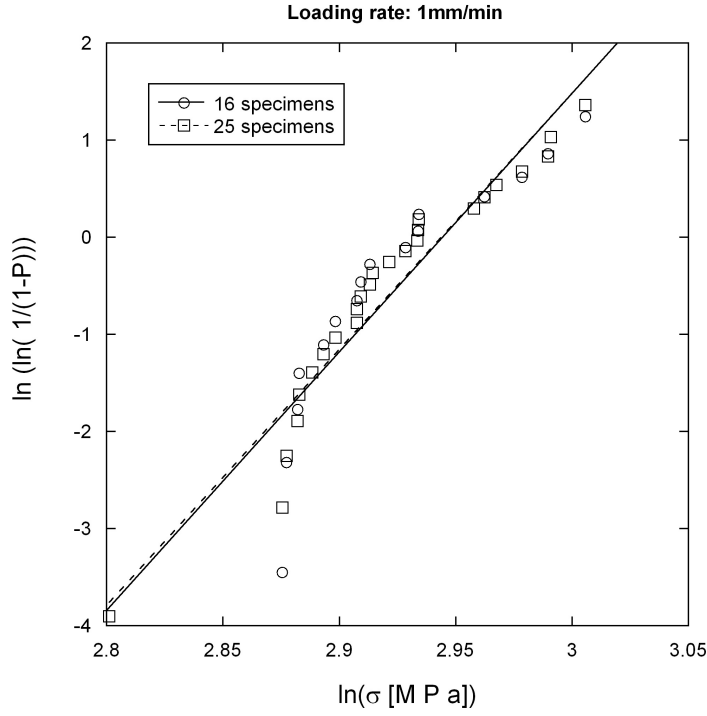


Figure 3: Same as Figure 2 showing only the measurements made at a loading rate of 1 mm/min. In addition to the data set containing 16 specimens, a second data set containing 25 specimens is shown. This second data set includes the measurements with the same 16 specimens as the first one, as well as 9 additional specimens whose dimensions have been determined with less accuracy (see text for details). The slopes of the two curves are similar. However, the second data set cannot be used for general purposes as it mixes specimens whose dimensions have not been measured with a same accuracy.

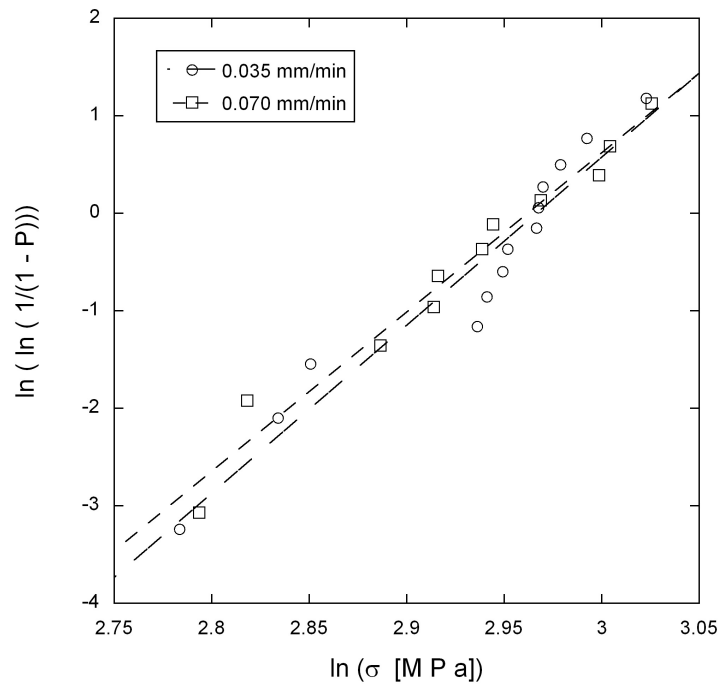


Figure 4 : Same as Figure 2, showing only the data from the two lowest loading rates for which Weibull's approach is appropriate. The slope of each line corresponds to the Weibull modulus  $m$  at the corresponding loading rate. It is equal to  $17.2 \pm 1.4$  and  $16.3 \pm 0.9$  for 0.035 mm/min and 0.070 mm/min, respectively. Thus, both loading rates lead to similar values of the modulus.

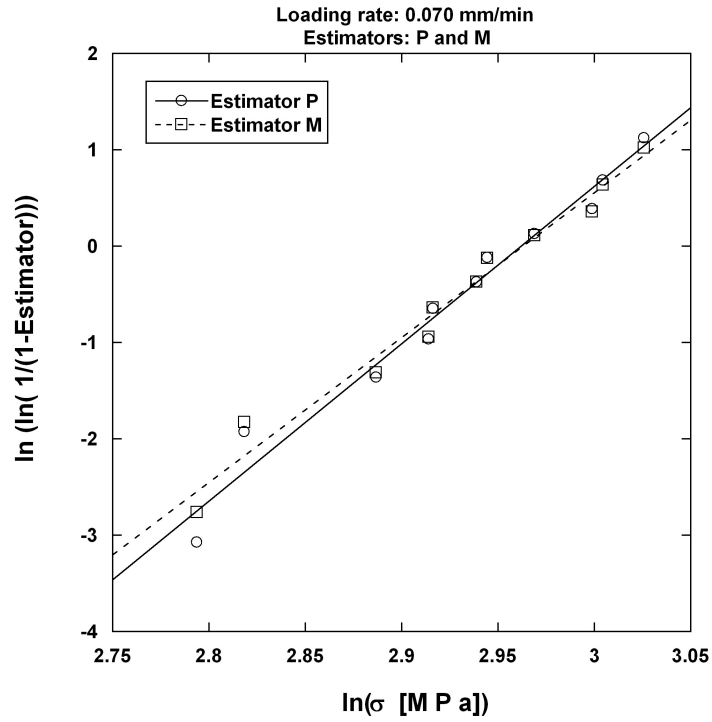


Figure 5 : Linear form of the cumulative probability of failure obtained with a loading rate of 0.070 mm/min. The fits obtained for the two estimators P (Eq. (4)) and M (Eq. (5)) are shown. The Weibull modulus  $m$  given by the slope of each line is equal to  $16.3 \pm 0.9$  and  $15.0 \pm 0.8$  from the estimator P and M, respectively.